

## **ELECTRONIC SUPPORTING INFORMATION**

# **Model Peptide Studies of Ag<sup>+</sup> Binding Sites from the Silver Resistance Protein SilE**

**V. Chabert,<sup>a</sup> M. Hologne,<sup>b</sup> O. Sénèque,<sup>c</sup> A. Crochet,<sup>d</sup> O. Walker<sup>b</sup> and K. M. Fromm<sup>a\*</sup>**

<sup>a.</sup> Univ. Fribourg, Department of Chemistry, Chemin du Musée 9, 1700 Fribourg, Switzerland. E-mail: katharina.fromm@unifr.ch

<sup>b.</sup> Univ. Lyon, CNRS, UCB Lyon 1, ENS-Lyon, Institut des Sciences Analytiques, UMR 5280, 5 rue de la Doua, 69100 Villeurbanne, France.

<sup>c.</sup> Univ. Grenoble Alpes, LCBM and CEA/BIG/CBM/PMB and CNRS, LCBM, UMR 5249, 38000 Grenoble, France.

<sup>d.</sup> Univ. Fribourg, Fribourg Center for Nanomaterials, FriMat, Chemin du Musée 9, 1700 Fribourg, Switzerland.

## **Table of contents**

Experimental Procedures .....	3
Determination of Ag <sup>+</sup> /peptides binding constants.....	4
AgHETM <sup>1</sup> H, <sup>13</sup> C-HSQC NMR spectra.....	8
Methionine oxidation assays.....	9
Silver-methionine solid state structure .....	11
Characterization of LP1 .....	14
References .....	16

## Experimental Procedures

**Solid-Phase Peptide Synthesis (SPPS).** Peptide models were synthesized by SPPS (Solid-Phase Peptide Synthesis) on a Rink-Amide resin (Novabiochem) on a 118 µmol scale.<sup>1</sup> The resin has been swelled in DCM (dichloromethane) during 30 min under stirring. 9-fluoromethoxy-carbonyl (Fmoc)-protected amino acids (Bachem) were coupled by using PyBOP (benzotriazol-1-yl-oxytrityrrolidinophosphonium hexafluorophosphate, Novabiochem) as coupling agent, DIPEA (N,N-diisopropylethylamine, Sigma-Aldrich) as organic base, and DMF (N,N'-dimethylformamide, Sigma-Aldrich) as solvent, during 30 min. After each coupling, a mixture of acetic anhydride (Acros Organics)/pyridine (Acros Organics)/DMF (1:2:7) has been added to the resin during 3 min in order to protect the unreacted functional groups. Fmoc deprotection steps were carried out by using 20% piperidine (Sigma-Aldrich) in DMF, three times during 3 min. The N-terminus was acetylated by using a mixture of acetic anhydride/pyridine/DMF (1:2:7) during 3 min. After each step, the solvent has been removed by filtration and the resin has been washed five times with DMF, and once with DCM. Side chain deprotection and peptide cleavage from the resin were carried out by adding 8 mL of a cocktail of 95.5% TFA (trifluoroacetic acid, Sigma-Aldrich), 1.5% EDT (ethane dithiol, Sigma-Aldrich), 1.5% TIS (triisopropylsilane, Sigma-Aldrich) and 1.5% water during 2h. The TFA has been evaporated under vacuum and the peptides were precipitated and washed 3 times with cold diethyl ether (Sigma-Aldrich). Peptides were dried and purified by semi-preparative reverse-phase HPLC (Waters 600) on a NUCLEODUR C18 HTec Column (Macherey-Nagel) with a linear gradient from 5% to 40% acetonitrile in water with 0.1% TFA, and then lyophilized. Characterization of the peptides was performed by ESI-MS (Bruker Esquire HCT) and <sup>1</sup>H NMR (Bruker Ascend 400 MHz), and the purity (> 95%) was controlled by analytical HPLC (Waters alliance).

**NMR spectroscopy.** Lyophilized peptides (1-2 mg) have been dissolved in 300 µL of D<sub>2</sub>O (Cambridge Isotope Laboratories) and the concentrations have been determined by UV-Vis spectroscopy. The molar absorptivity at 205 nm ( $\epsilon_{205}$ ) of each peptide is given by the modified formula (from Anthis *et al.*<sup>2</sup>):

$$\epsilon_{205} = \sum (\epsilon_i n_i) + \epsilon_{bb} \times r$$

where for each amino acid *i*,  $\epsilon_i$  is the molar absorptivity of the amino acid side chain (from Goldfarb *et al.*<sup>3</sup> for all values, except for glutamine and asparagine values, which come from Saidel *et al.*<sup>4</sup>) and  $n_i$  is the number of times that this amino acid appears in the peptide sequence.  $\epsilon_{bb}$  is the molar absorptivity of a backbone peptide bond, and *r* is the number of residues in the peptide sequence. Peptide solutions (500 µM) were then prepared in a deuterated HEPES (4-(2-hydroxyethyl)-1-piperazineethanesulfonic acid) buffer (20 mM, pD 7.8), and <sup>1</sup>H NMR titrations were performed on a Bruker Ascend 400 MHz by adding increasing amounts of AgClO<sub>4</sub> deuterated solution of which the concentration (48.0 mM) has been previously determined by ICP analysis. Titration experiments using imidazole-d4 as a competitor have been performed in the above-mentioned conditions, using the imidazole-d4 (3-25 mM, pD 7.8) as buffer instead of HEPES. The titration curves were fitted using the program DynaFit<sup>5</sup>, with the binding constants of [Ag(imidazole)<sub>n</sub>]<sup>+</sup> (*n* = 1, 2) complexes (LogK<sub>ass</sub> = 2.96 and 6.71 for the 1:1 and 1:2 complexes respectively) determined by Czoik *et al.*<sup>6</sup>. <sup>1</sup>H, <sup>13</sup>C-HSQC spectra where measured with peptide samples of ca. 50 mM in D<sub>2</sub>O, before and after addition of 2 eq. of AgClO<sub>4</sub> deuterated solution (0.96 M). DOSY experiments were recorded using stimulated echo employing bipolar gradients and 3-9-19 pulse sequence for water suppression ( $\Delta$  = 200 ms,  $\delta$  = 1ms, 16384 x 32 points, T = 303 K) in the case of the free and complexed form of LP1.

**CD spectroscopy.** The concentration determination of LP1 solutions has been performed as previously described for NMR experiments. The measurements have been performed on a Jasco J-715 spectropolarimeter.

**Oxidation assays.** Lyophilized peptides (1-2 mg) have been dissolved in bidistilled water in order to reach a concentration of ca. 1 mM. Then, pH values have been adjusted to 7 by adding a few drops of NaOH solution (1 M). AgClO<sub>4</sub> (1 eq.) has been then added to half of the solution volumes. Each sample has been measured by HPLC analysis (Waters alliance, Linear gradient: 5% to 30% acetonitrile in water with 0.1% TFA in 15 min) and ESI-MS analysis (Bruker Esquire HCT), before and after addition of H<sub>2</sub>O<sub>2</sub> (100 eq.) during 1h.

**{[Ag<sub>2</sub>(L-Methionine)<sub>4</sub>](NO<sub>3</sub>)<sub>2</sub>, 2H<sub>2</sub>O}<sub>n</sub> crystallization.** Silver nitrate (85 mg, 0.5 mmol, Acros Organics) and L-methionine (149 mg, 1 mmol, Sigma-Aldrich) were added to a NMR tube containing 500 μL of D<sub>2</sub>O. The tube has been sonicated and heated until a clear solution was obtained. The sample has been stored in the dark for 1 day, and single crystals of {[Ag<sub>2</sub>(L-Methionine)<sub>4</sub>](NO<sub>3</sub>)<sub>2</sub>, 2H<sub>2</sub>O}<sub>n</sub> were obtained. Data collection for single crystal X-ray crystallography has been performed using Mo-Kα radiation (0.71073 Å) at 200(2) K with a STOE IPDS II diffractometer equipped with an Oxford Cryosystem open flow cryostat. The structure has been solved and refined using full-matrix least-squares on *F*<sup>2</sup> with the SHELXL package<sup>7</sup>. The crystal has been mounted on loops and all geometric and intensity data were taken from one single crystal. All heavy atoms have been refined anisotropically. Crystallographic data has been deposited with the Cambridge Crystallographic Data Center, 12 Union Road, Cambridge CB21EZ, UK. Copies of the data can be obtained on quoting the depositing numbers CCDC 1547635 (Fax: +44-1223-336-033; E-mail: deposit@ccdc.cam.ac.uk).

### Determination of Ag<sup>+</sup>/peptides binding constants

Silver binding constants (LogK<sub>ass</sub>) of each complex have been determined from Ag<sup>+</sup> titrations of the peptides in competition with imidazole-d4. Figures S1-S8 show the plot of Met-H<sup>ε</sup>, His-H<sup>δ2</sup> and/or His-H<sup>ε1</sup> (when Δδ ≥ 0.05 ppm) <sup>1</sup>H NMR resonances shifts obtained during the competition experiments and the fits obtained using the program Dynafit<sup>5</sup>.

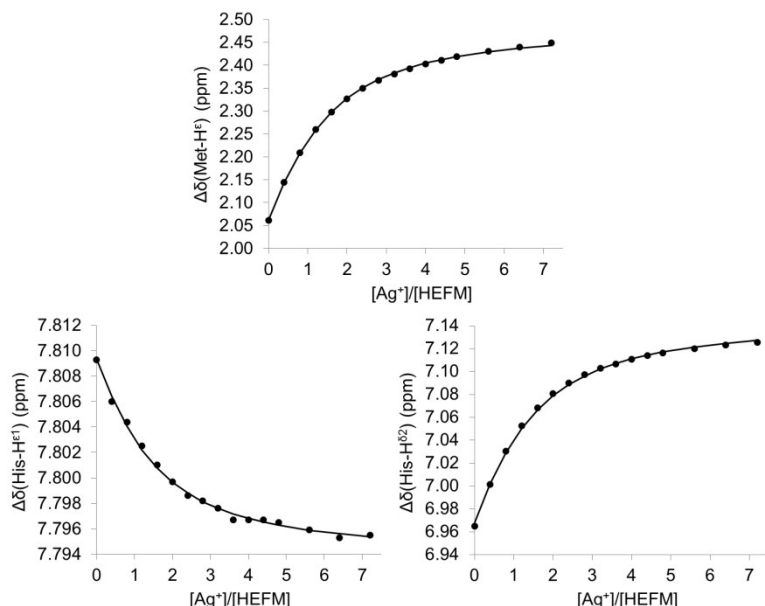


**Figure S1.** Plots of the histidine and methionine <sup>1</sup>H resonances shift by addition of AgClO<sub>4</sub> (0 to 4.36 mM) to a solution of HEFM (500 μM) in competition with imidazole-d4 (17.15 mM, pD 7.8). The solid lines correspond to the fits obtained with DynaFit.<sup>5</sup>

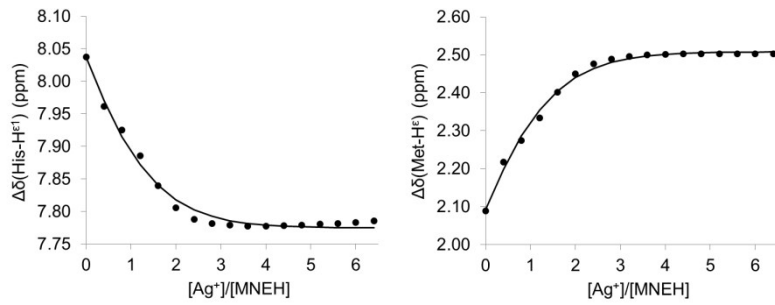


**Figure S2.** Plots of the histidine and methionine  $^1\text{H}$  resonances shift by addition of  $\text{AgClO}_4$  (0 to 4.36 mM) to a solution of MNEH (500  $\mu\text{M}$ ) in competition with imidazole-d4 (3.32 mM, pD 7.8). The solid lines correspond to the fits obtained with DynaFit.<sup>5</sup>

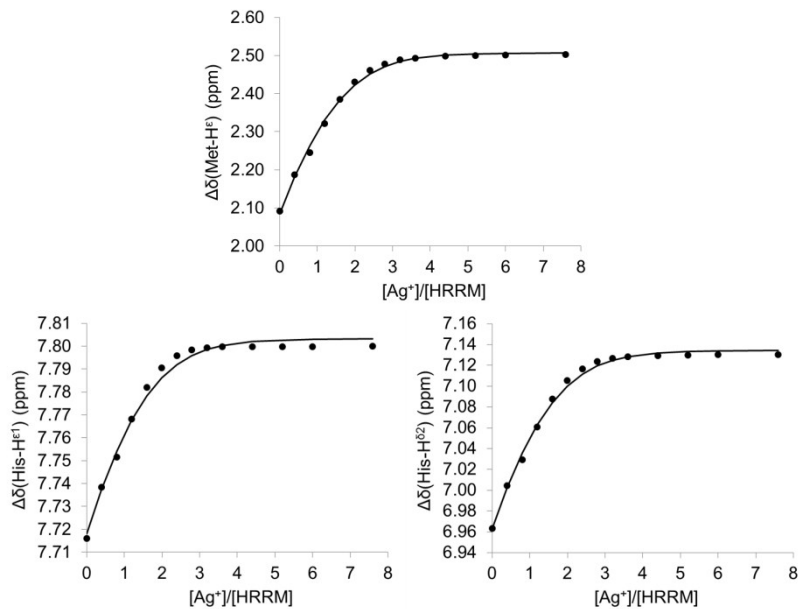


**Figure S3.** Plots of the histidine and methionine  $^1\text{H}$  resonances shift by addition of  $\text{AgClO}_4$  (0 to 4.36 mM) to a solution of HRRM (500  $\mu\text{M}$ ) in competition with imidazole-d4 (3.18 mM, pD 7.8). The solid lines correspond to the fits obtained with DynaFit.<sup>5</sup>

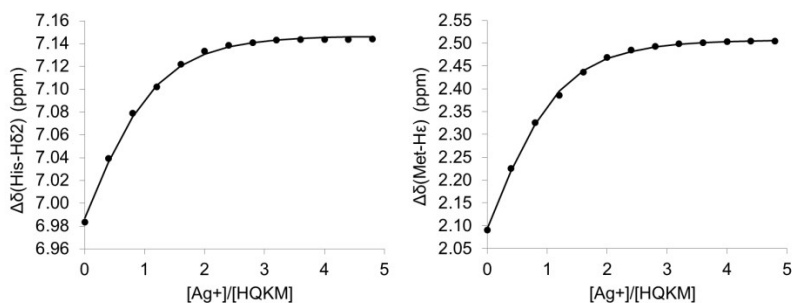


**Figure S4.** Plots of the histidine and methionine  $^1\text{H}$  resonances shift by addition of  $\text{AgClO}_4$  (0 to 4.36 mM) to a solution of HQKM (500  $\mu\text{M}$ ) in competition with imidazole-d4 (3.43 mM, pD 7.8). The solid lines correspond to the fits obtained with DynaFit.<sup>5</sup>

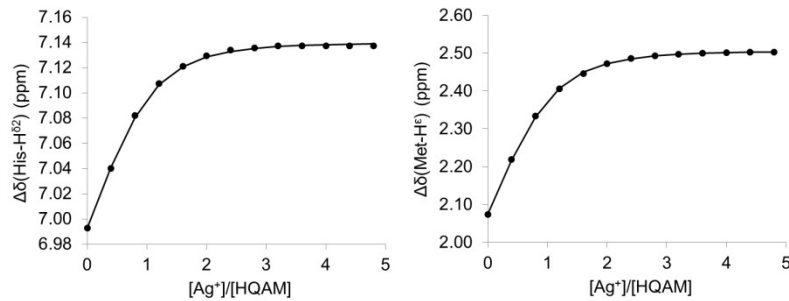


**Figure S5.** Plots of the histidine and methionine  $^1\text{H}$  resonances shift by addition of  $\text{AgClO}_4$  (0 to 4.36 mM) to a solution of HQAM (500  $\mu\text{M}$ ) in competition with imidazole-d4 (3.46 mM, pD 7.8). The solid lines correspond to the fits obtained with DynaFit.<sup>5</sup>

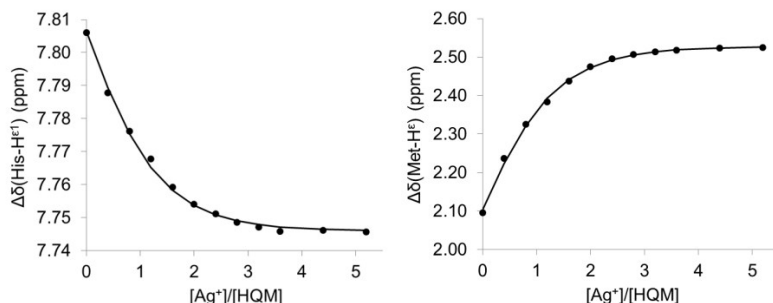


**Figure S6.** Plots of the histidine and methionine  $^1\text{H}$  resonances shift by addition of  $\text{AgClO}_4$  (0 to 4.36 mM) to a solution of HQM (500  $\mu\text{M}$ ) in competition with imidazole-d4 (3.35 mM, pD 7.8). The solid lines correspond to the fits obtained with DynaFit.<sup>5</sup>

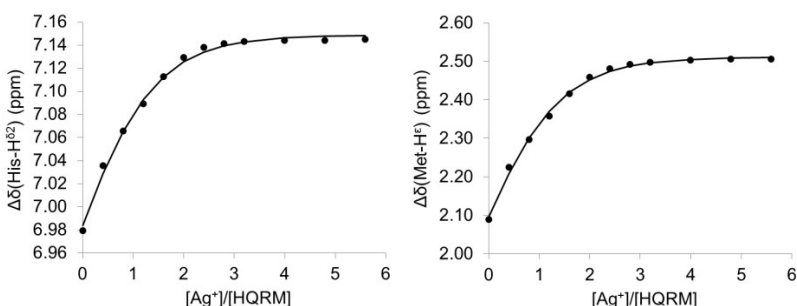


**Figure S7.** Plots of the histidine and methionine  $^1\text{H}$  resonances shift by addition of  $\text{AgClO}_4$  (0 to 4.36 mM) to a solution of HQRM (500  $\mu\text{M}$ ) in competition with imidazole-d4 (3.2 mM, pD 7.8). The solid lines correspond to the fits obtained with DynaFit.<sup>5</sup>

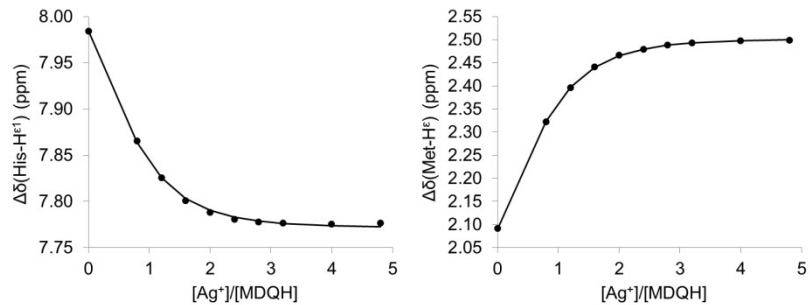


**Figure S8.** Plots of the histidine and methionine  $^1\text{H}$  resonances shift by addition of  $\text{AgClO}_4$  (0 to 4.36 mM) to a solution of MDQH (500  $\mu\text{M}$ ) in competition with imidazole-d4 (3.25 mM, pD 7.8). The solid lines correspond to the fits obtained with DynaFit.<sup>5</sup>

**Table S1.** Comparison of the binding constants ( $\text{Log}K_{\text{ass}} \pm 0.1$ ) individually determined from  $\text{His}-\text{H}^{\delta 1}$ ,  $\text{His}-\text{H}^{\delta 2}$  and  $\text{Met}-\text{H}^{\epsilon}$   $^1\text{H}$  NMR shifts.

Model	$ \Delta\delta(\text{His}-\text{H}^{\delta 1}) ^{[a]}$	$\text{Log}K_{\text{ass}}(\text{His}-\text{H}^{\delta 1})^{[b]}$	$ \Delta\delta(\text{His}-\text{H}^{\delta 2}) ^{[a]}$	$\text{Log}K_{\text{ass}}(\text{His}-\text{H}^{\delta 2})^{[b]}$	$ \Delta\delta(\text{Met}-\text{H}^{\epsilon}) ^{[a]}$	$\text{Log}K_{\text{ass}}(\text{Met}-\text{H}^{\epsilon})^{[b]}$
HQM	0.055	5.5	-	-	0.432	5.6
MDQH	0.216	5.8	0.004	-	0.415	5.7
MNEH	0.214	5.4	0.015	-	0.424	5.4
HETM	0.118	6.3	0.107	6.5	0.413	6.4
HEFM	0.099	6.5	0.140	6.6	0.447	6.6
HQKM	0.017	-	0.156	5.8	0.414	5.7
HQRM	0.041	-	0.167	5.5	0.417	5.5
HQAM	0.008	-	0.147	6.0	0.414	5.9
HRRM	0.081	5.4	0.165	5.3	0.406	5.2

[a] The  $^1\text{H}$  NMR shifts ( $\Delta\delta$ ) correspond to maximal values of the peptides titration by  $\text{AgClO}_4$ . [b]  $\text{Log}K_{\text{ass}}$  values are extracted from competition experiments using imidazole-d4 (using  $\text{Ag(imidazole)}_n$  ( $n = 1, 2$ ) binding constants from Czoik et al.).<sup>6</sup>

## AgHETM $^1\text{H}$ , $^{13}\text{C}$ -HSQC NMR spectra

The comparison of  $^1\text{H}$ ,  $^{13}\text{C}$ -HSQC NMR spectra of the apo- and holo-forms of each model peptide allowed to find out which amino acid were involved in the  $\text{Ag}^+$  coordination sphere. Indeed,  $^{13}\text{C}$  NMR chemical shift are less sensitive to conformational changes and can therefore attest to the  $\text{Ag}^+$  binding to the different side chains when nearby  $^{13}\text{C}$  resonances are altered<sup>8</sup>. This highlighted a methionine and histidine involvement in  $\text{Ag}^+$  coordination in each model and a glutamate participation in AgHETM and AgHEFM (Figure S9).

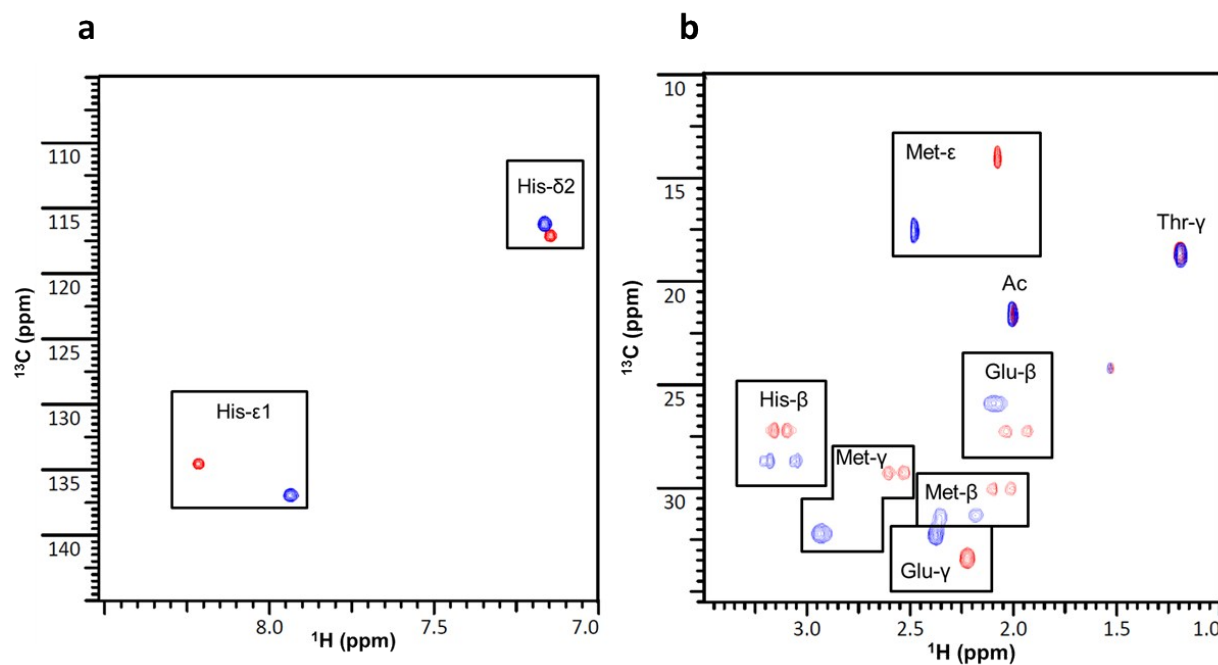


**Figure S9.**  $^1\text{H}$ ,  $^{13}\text{C}$ -HSQC NMR spectra of HETM (red) and AgHETM (blue). (a) The His- $\text{C}^{\delta 2}$  resonance at 117 ppm in each spectrum indicates a predominance of the His- $\text{N}^{\varepsilon 2}$ -H tautomer. (b) The Glu- $\text{C}^\beta$  and Glu- $\text{C}^\gamma$  resonances shift suggests a glutamate participation in  $\text{Ag}^+$  coordination. The peptide concentration is 50 mM in  $\text{D}_2\text{O}$ .

## Methionine oxidation assays

Due to their sulfur containing side chain, the methionine residues are highly oxidizable in presence of reactive oxygen species (ROS)<sup>9,10</sup>. To explore this sensitivity in our models and its effect on silver complexation, oxidation assays were performed by incubating the models in presence of an excess of hydrogen peroxide during 1h. Using this procedure, all free peptides were oxidized to sulfoxide, respectively in one case into sulfone. These results have been confirmed by both ESI-MS and analytical HPLC (Table S2). For instance, the ESI-MS spectrum of HETM before  $\text{H}_2\text{O}_2$  treatment shows two peaks which correspond to sodium adducts of the reduced peptide ( $[\text{HETM}+\text{Na}]^+$  and  $[\text{HETM}+2\text{Na}-\text{H}]^+$ ) (Figure S10a), while after  $\text{H}_2\text{O}_2$  treatment, the spectrum only shows peaks of the sulfoxide species ( $[\text{HETM(O)}+\text{Na}]^+$  and  $[\text{HETM(O)}+2\text{Na}-\text{H}]^+$ ) (Figure S10b). Moreover, the HPLC analysis confirms the full oxidation of the peptide by  $\text{H}_2\text{O}_2$  (Figure S10e). However, when bound to silver, the same model peptide can no longer be oxidized by  $\text{H}_2\text{O}_2$ . Indeed, ESI-MS spectra and HPLC chromatograms of all the silver bound model peptides are identical before and after  $\text{H}_2\text{O}_2$  treatment. The two ESI-MS spectra show the same species (e.g.  $[\text{AgHETM}]^+$  and  $[\text{AgHETM}+\text{Na}-\text{H}]^+$ ) (Figure S10c-d) and the HPLC chromatograms present the same retention time before and after treatment with  $\text{H}_2\text{O}_2$  (Figure S10f).

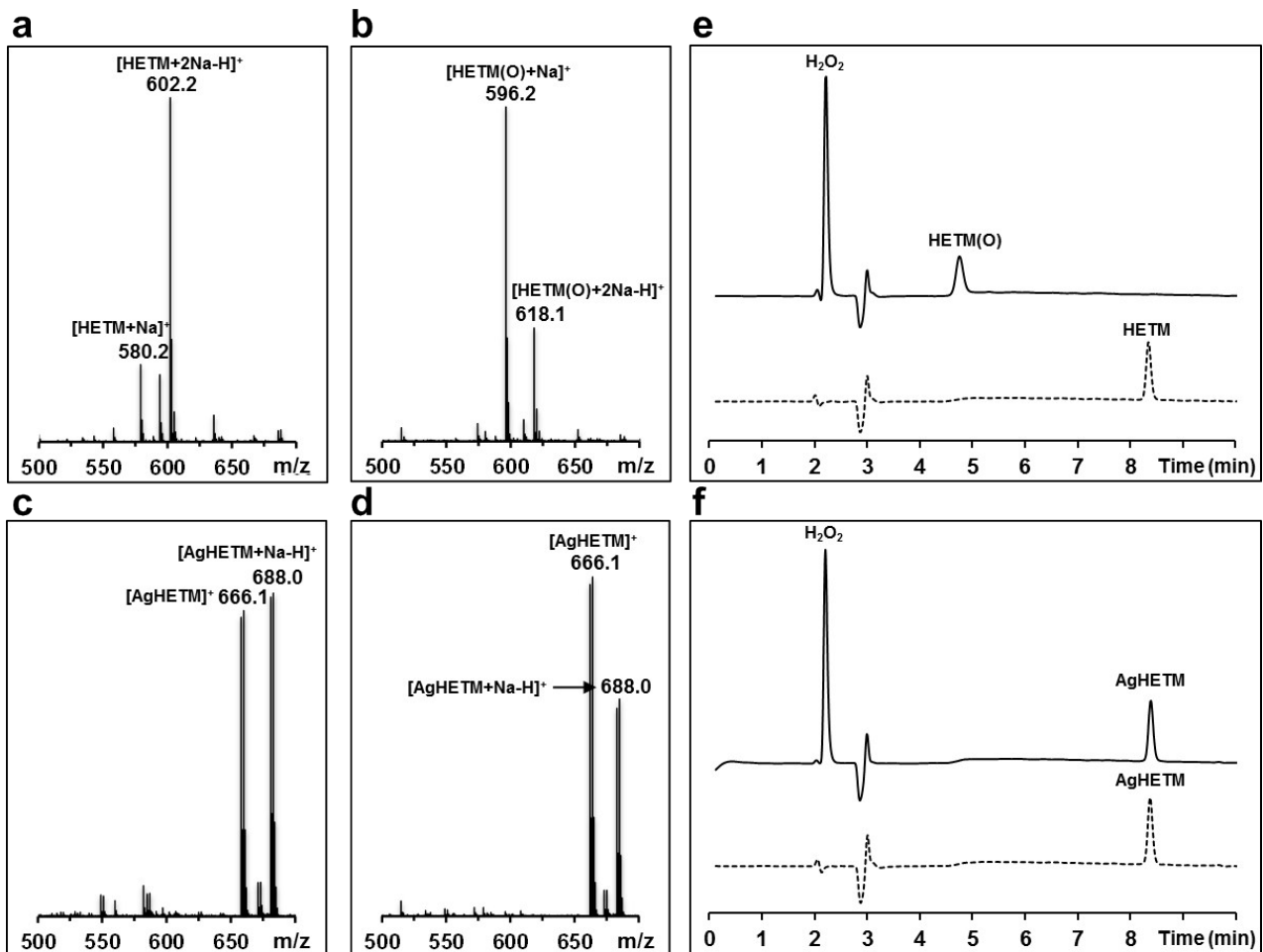


**Figure S10.** Methionine oxidation assays. (a-b) ESI-MS analysis of HETM (1 mM) before (a) and after (b) a one hour incubation with  $\text{H}_2\text{O}_2$  (100 mM). (c-d) ESI-MS analysis of AgHETM (1 mM) before (d) and after (e) a one hour incubation with  $\text{H}_2\text{O}_2$  (100 mM). (e-f) HPLC monitoring of HETM (e) and AgHETM (f) oxidation assays before (dashed line) and after (solid line)  $\text{H}_2\text{O}_2$  incubation. (HPLC gradient: 5% to 30% acetonitrile in water with 0.1% TFA in 15 min).

**Table S2.** ESI-MS observed species and HPLC retention times of the models before and after incubation with H<sub>2</sub>O<sub>2</sub>.

Model	ESI-MS before H <sub>2</sub> O <sub>2</sub> (m/z)	ESI-MS before H <sub>2</sub> O <sub>2</sub> (species)	ESI-MS after H <sub>2</sub> O <sub>2</sub> (m/z)	ESI-MS after H <sub>2</sub> O <sub>2</sub> (species)	HPLC retention time before H <sub>2</sub> O <sub>2</sub> (min)	HPLC retention time after H <sub>2</sub> O <sub>2</sub> (min)
MDQH	593.2	[MDQH+Na] <sup>+</sup>	609.1	[MDQH(O)+Na] <sup>+</sup>	8.3	2.2
	615.2	[MDQH+2Na-H] <sup>+</sup>	631.1	[MDQH(O)+2Na-H] <sup>+</sup>		
HETM	580.2	[HETM+Na] <sup>+</sup>	596.2	[HETM(O)+Na] <sup>+</sup>	8.4	4.7
	602.2	[HETM+2Na-H] <sup>+</sup>	618.1	[HETM(O)+2Na-H] <sup>+</sup>		
HEFM	626.2	[HEFM+Na] <sup>+</sup>	642.2	[HEFM(O)+Na] <sup>+</sup>	9.2	7.3
	648.2	[HEFM+2Na-H] <sup>+</sup>	658.2	[HEFM(OO)+Na] <sup>+</sup>		
HRRM	640.3	[HRRM+H] <sup>+</sup>	656.3	[HRRM(O)+H] <sup>+</sup>	8.8	6.2
	320.7	[HRRM+2H] <sup>2+</sup>	328.6	[HRRM(O)+2H] <sup>2+</sup>		
	754.2	[HRRM+H+TFA] <sup>+</sup>	770.2	[HRRM(O)+H+TFA] <sup>+</sup>		
HQM	478.1	[HQM+Na] <sup>+</sup>	494.1	[HQM(O)+Na] <sup>+</sup>	7.1	3.6
HQKM	584.2	[HQKM+H] <sup>+</sup>	600.3	[HQKM(O)+H] <sup>+</sup>	7.5	4.0
	606.2	[HQKM+Na] <sup>+</sup>	622.3	[HQKM(O)+Na] <sup>+</sup>		
HQRM	612.2	[HQRM+H] <sup>+</sup>	628.3	[HQRM(O)+H] <sup>+</sup>	7.9	5.0
MNEH	615.2	[MNEH+2Na-H] <sup>+</sup>	631.2	[MNEH(O)+2Na-H] <sup>+</sup>	8.3	4.2
HQAM	549.1	[HQAM+Na] <sup>+</sup>	565.2	[HQAM(O)+Na] <sup>+</sup>	7.7	4.1

**Table S3.** ESI-MS observed species and HPLC retention times of the model complexes before and after incubation with H<sub>2</sub>O<sub>2</sub>.

Model	ESI-MS before H <sub>2</sub> O <sub>2</sub> (m/z)	ESI-MS before H <sub>2</sub> O <sub>2</sub> (species)	ESI-MS after H <sub>2</sub> O <sub>2</sub> (m/z)	ESI-MS after H <sub>2</sub> O <sub>2</sub> (species)	HPLC retention time before H <sub>2</sub> O <sub>2</sub> (min)	HPLC retention time after H <sub>2</sub> O <sub>2</sub> (min)
AgMDQH	699.1/701.1	[AgMDQH+Na-H] <sup>+</sup>	Idem	Idem	8.3	Idem
AgHETM	664.1/666.1	[AgHETM] <sup>+</sup>	Idem	Idem	8.4	Idem
	686.1/688.0	[AgHETM+Na-H] <sup>+</sup>				
AgHEFM	710.2/712.1	[AgHEFM] <sup>+</sup>	Idem	Idem	9.4	Idem
	732.1/734.1	[AgHEFM+Na-H] <sup>+</sup>				
AgHRRM	746.2/748.2	[AgHRRM] <sup>+</sup>	Idem	Idem	8.8	Idem
	373.7/374.6	[AgHRRM+H] <sup>2+</sup>				
AgHQM	562.0/564.0	[AgHQM] <sup>+</sup>	Idem	Idem	7.1	Idem
AgHQKM	690.1/692.1	[AgHQKM] <sup>+</sup>	Idem	Idem	7.3	Idem
	345.6/346.6	[AgHQKM+H] <sup>2+</sup>				
AgHQRM	718.1/720.1	[AgHQRM] <sup>+</sup>	Idem	Idem	7.9	Idem
	359.7/360.6	[AgHQRM+H] <sup>2+</sup>				
AgMNEH	699.1/701.0	[AgMNEH+Na-H] <sup>+</sup>	Idem	Idem	8.3	Idem
AgHQAM	633.1/635.0	[AgHQAM] <sup>+</sup>	Idem	Idem	7.7	Idem

## Silver-methionine solid state structure

The complex  $\{[\text{Ag}_2(\text{L-Methionine})_4](\text{NO}_3)_2 \bullet 2\text{H}_2\text{O}\}_n$  crystallizes in the monoclinic  $P2_1$  space group and contains two independent silver ions. Each metal ion is coordinated in a trigonal planar fashion (Sum of angles :  $\Sigma\text{Ag}1 = 360^\circ$ ;  $\Sigma\text{Ag}2 = 352.2^\circ$ ) by the carboxylate group of one methionine ( $\text{Ag}1-\text{O}4 = 2.34(1)$  Å,  $\text{Ag}2-\text{O}1 = 2.34(2)$  Å) and by the thioether moieties of two other methionine ligands ( $\text{Ag}1-\text{S}1 = 2.454(7)$  Å,  $\text{Ag}1-\text{S}4 = 2.487(6)$  Å,  $\text{Ag}2-\text{S}2\#1 = 2.503(7)$  Å,  $\text{Ag}2-\text{S}3 = 2.538(6)$  Å; #1:  $x+1, y, z$ ). The calculated bond valences evidence a stronger binding of sulfur atoms to the silver cation ( $S_{\text{Ag}1-\text{S}1} = 0.40$ ,  $S_{\text{Ag}1-\text{S}4} = 0.37$ ,  $S_{\text{Ag}2-\text{S}2} = 0.35$ ,  $S_{\text{Ag}2-\text{S}3} = 0.32$ ) than of the oxygen atoms ( $S_{\text{Ag}1-\text{O}4} = 0.26$ ,  $S_{\text{Ag}2-\text{O}1} = 0.26$ )<sup>11</sup>. Each metal coordination sphere is complemented by two weak bonds ( $S_{\text{Ag}1-\text{O}3} = 0.04$ ,  $S_{\text{Ag}1-\text{O}3\#1} = 0.06$ ,  $S_{\text{Ag}2-\text{O}2} = 0.07$ ,  $S_{\text{Ag}2-\text{S}2} = 0.05$ ).

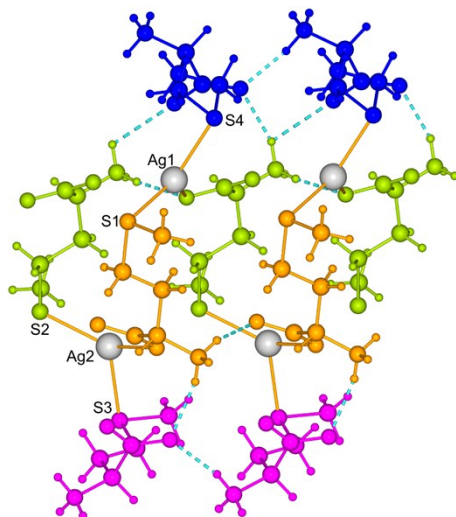


**Figure S11.** 1D coordination polymer formed by the  $\{[\text{Ag}_2(\text{L-Methionine})_4](\text{NO}_3)_2 \bullet 2\text{H}_2\text{O}\}_n$  complex along the  $\alpha$  axis. The complex forms a helical 1D coordination polymer along the  $\alpha$  axis. The coordination spheres of the two silver ions are completed by a third methionine on each side of the helix.

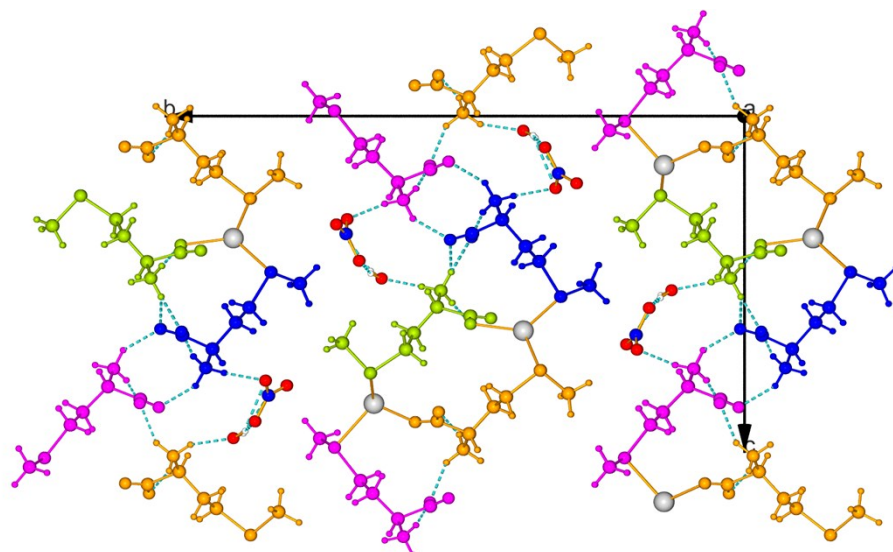


**Figure S12.** Crystal packing of the  $\{[\text{Ag}_2(\text{L-Methionine})_4](\text{NO}_3)_2 \bullet 2\text{H}_2\text{O}\}_n$  complex. The helix is stabilized by intra- and intermolecular hydrogen bonds (dash bonds). The channels between the helices are occupied by nitrates and water molecules forming additional hydrogen bonds.

**Table S4.** Crystal data and structure refinement for {[Ag<sub>2</sub>(L-Methionine)<sub>4</sub>](NO<sub>3</sub>)<sub>2</sub>•2H<sub>2</sub>O}<sub>n</sub>.

Empirical formula	C <sub>20</sub> H <sub>48</sub> Ag <sub>2</sub> N <sub>6</sub> O <sub>16</sub> S <sub>4</sub>	
Formula weight	972.62	
Temperature	200(2) K	
Wavelength	0.71073 Å	
Crystal system	Monoclinic	
Space group	P 21	
Unit cell dimensions	$a = 5.0810(3)$ Å $b = 24.7309(12)$ Å $c = 14.5097(10)$ Å	$\alpha = 90^\circ$ $\beta = 99.007(5)^\circ$ $\gamma = 90^\circ$
Volume	1800.77(19) Å <sup>3</sup>	
Z	2	
Density (calculated)	1.794 Mg/m <sup>3</sup>	
Absorption coefficient	1.393 mm <sup>-1</sup>	
F(000)	992	
Crystal size	0.480 x 0.180 x 0.030 mm <sup>3</sup>	
Theta range for data collection	1.421 to 25.189°.	
Index ranges	-6≤h≤6, -29≤k≤29, 0≤l≤17	
Reflections collected	6406	
Independent reflections	6406 [R(int) = 0.1138]	
Completeness to theta = 25.189°	99.2 %	
Absortion correction	Integration	
Max. and min. transmission	0.9681 and 0.7492	
Refinement method	Full-matrix least-squares on F <sup>2</sup>	
Data / restraints / parameters	6406 / 59 / 423	
Goodness-of-fit on F <sup>2</sup>	1.019	
Final R indices [I>2sigma(I)]	R1 = 0.0864, wR2 = 0.2272	
R indices (all data)	R1 = 0.1164, wR2 = 0.2525	
Absolute structure parameter	0.02(3)	
Extinction coefficient	n/a	
Largest diff. peak and hole	1.651 and -1.109 e.Å <sup>-3</sup>	

Reffined as a 2-component perfect twin. H atoms on heteroatoms not refined.

**Table S5.** Bond lengths [Å] and angles [°] for {[Ag<sub>2</sub>(L-Methionine)<sub>4</sub>](NO<sub>3</sub>)<sub>2</sub>•2H<sub>2</sub>O}<sub>n</sub>.

Ag(1)-O(4)	2.339(14)	Ag(2)-O(2)	2.85(2)
Ag(1)-S(1)	2.454(7)	Ag(2)-S(2)	3.224(6)
Ag(1)-S(4)	2.487(6)	O(4)-Ag(1)-S(1)	122.4(4)
Ag(1)-O(3)	3.02(2)	O(4)-Ag(1)-S(4)	114.9(4)
Ag(1)-O(3)#1	2.86(2)	S(1)-Ag(1)-S(4)	122.6(2)
Ag(2)-O(1)	2.336(16)	O(1)-Ag(2)-S(2)#1	134.9(5)
Ag(2)-S(2)#1	2.503(6)	O(1)-Ag(2)-S(3)	99.5(5)
Ag(2)-S(3)	2.538(6)	S(2)#1-Ag(2)-S(3)	117.8(2)

Symmetry transformations used to generate equivalent atoms: #1 x+1,y,z #2 x-1,y,z

**Table S6.** Hydrogen bonds for  $\{\text{Ag}_2(\text{L-Methionine})_4\}(\text{NO}_3)_2 \bullet 2\text{H}_2\text{O}\}_{\text{n}}$  [ $\text{\AA}$  and  $^{\circ}$ ].

D-H...A	d(D-H)	d(H...A)	d(D...A)	$\angle(\text{DHA})$
N(1)-H(1A)...O(6)	0.91	2.01	2.81(2)	145.1
N(1)-H(1B)...O(16)#3	0.91	2.00	2.85(3)	155.8
N(1)-H(1C)...O(2)#2	0.91	1.90	2.78(2)	161.0
N(2)-H(2A)...O(4)#2	0.91	1.91	2.81(2)	167.7
N(2)-H(2B)...O(7)#2	0.91	2.47	2.92(2)	110.7
N(2)-H(2B)...O(8)	0.91	1.98	2.85(2)	158.7
N(2)-H(2C)...O(15)	0.91	1.88	2.79(3)	179.5
N(3)-H(3C)...O(6)#1	0.91	1.88	2.76(2)	160.4
N(3)-H(3D)...O(7)#4	0.91	1.95	2.76(3)	147.1
N(3)-H(3E)...O(11)#5	0.91	2.02	2.92(3)	170.1
N(4)-H(4C)...O(5)#6	0.91	2.00	2.82(3)	149.9
N(4)-H(4D)...O(13)#1	0.91	2.06	2.97(2)	175.8
N(4)-H(4E)...O(8)#1	0.91	1.88	2.75(2)	159.7
O(15)-H(15D)...O(9)#2	0.87	2.01	2.84(3)	157.4
O(15)-H(15D)...O(10)#2	0.87	2.60	3.37(3)	146.6
O(15)-H(15E)...O(9)	0.87	1.95	2.79(3)	163.0
O(16)-H(16A)...O(12)	0.87	1.99	2.79(3)	154
O(16)-H(16B)...N(6)#1	0.87	2.57	3.38(2)	155
O(16)-H(16B)...O(12)#1	0.87	1.95	2.80(3)	165.5
O(16)-H(16B)...O(13)#1	0.87	2.521	3.12(2)	127.5

Symmetry transformations used to generate equivalent atoms: #1 x+1,y,z #2 x-1,y,z #3 x,y,z+1 #4 x+1,y,z+1 #5 x+2,y,z+1 #6 x-1,y,z-1

## Characterization of LP1

A 14-amino acid peptide (LP1: Ac-AHQKMVESHQRM MG-NH<sub>2</sub>) containing two HX<sub>2</sub>M motifs has been synthesized and studied for its interaction with silver ions. To confirm the stoichiometry of the Ag<sup>+</sup>/LP1 complex, DOSY experiments were recorded in the case of the free and complexed form. The resulting diffusion constants show similar values in the case of the free and complexed form, indicating that there is no dimerization of LP1 in presence of silver ions (Figure S14).

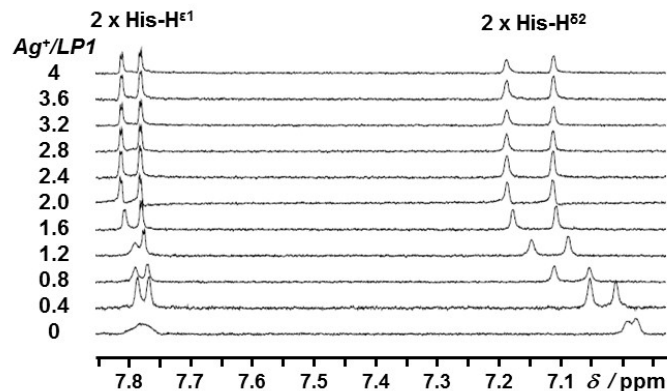


**Figure S13.** LP1 <sup>1</sup>H NMR titration. Histidine imidazole <sup>1</sup>H resonances (His-H<sup>ε1</sup>, His-H<sup>δ2</sup>) shift by addition of AgClO<sub>4</sub> (0 to 2 mM) to a solution of LP1 (500  $\mu$ M) in deuterated HEPES buffer (20 mM, pD 7.8).

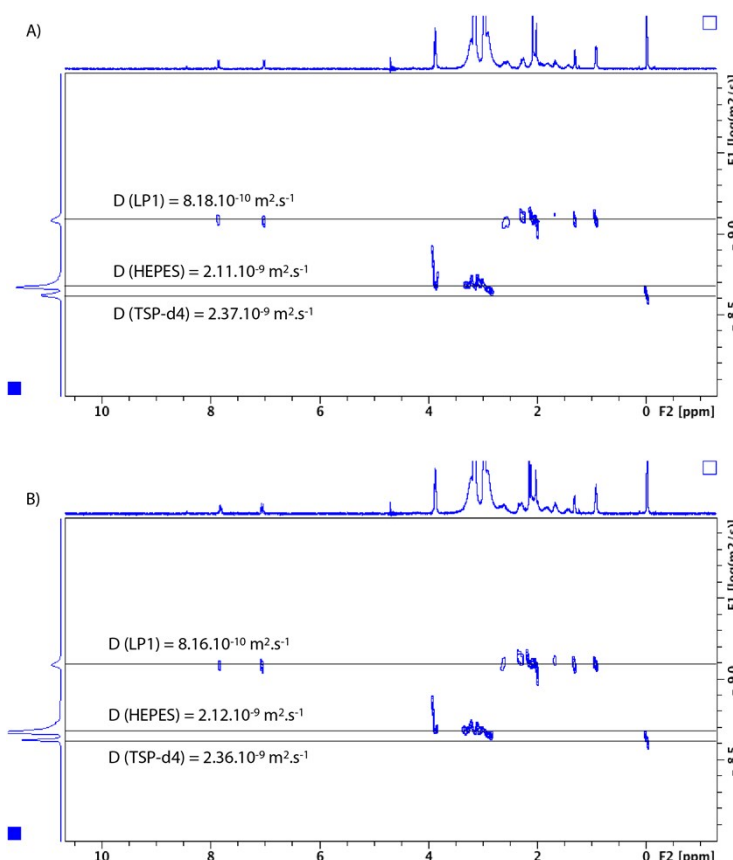


**Figure S14.** DOSY experiments of apo-LP1 (A) and holo-LP1 (B). Addition of AgClO<sub>4</sub> (8 mM) to a solution of LP1 (2 mM, HEPES 20 mM, pD 7.4) induces no significant changes in diffusion constant indicating that LP1 doesn't oligomerize to a dimer when complexed to silver ions. Data were processed using DOSY module of Topspin 3.2.

## References

- 1 R. B. Merrifield, *J. Am. Chem. Soc.*, 1963, **85**, 2149.
- 2 N. J. Anthis and G. M. Clore, *Protein Sci.*, 2013, **22**, 851.
- 3 A. R. Goldfarb, *J. Biol. Chem.*, 1951, **193**, 397.
- 4 L. J. Saidel, *J. Biol. Chem.*, 1952, **197**, 285.
- 5 P. Kuzmič, *Anal. Biochem.*, 1996, **237**, 260.
- 6 R. Czoik, A. Heintz, E. John and W. Marczak, *Acta Phys. Pol. A*, 2008, **114**, 51.
- 7 G. M. Sheldrick, *Acta Crystallogr. Sect. C Struct. Chem.*, 2015, **71**, 3.
- 8 B. Bersch et al., *Biochemistry*, 2011, **50**, 2194.
- 9 E. Cabiscol, J. Tamarit and J. Ros, *Int. Microbiol.*, 2000, **3**, 3.
- 10 J.-W. Chu and B. L. Trout, *J. Am. Chem. Soc.*, 2004, **126**, 900.
- 11 D. Altermatt, I. D. Brown and IUCr, *Acta Crystallogr. Sect. B Struct. Sci.*, 1985, **41**, 240.